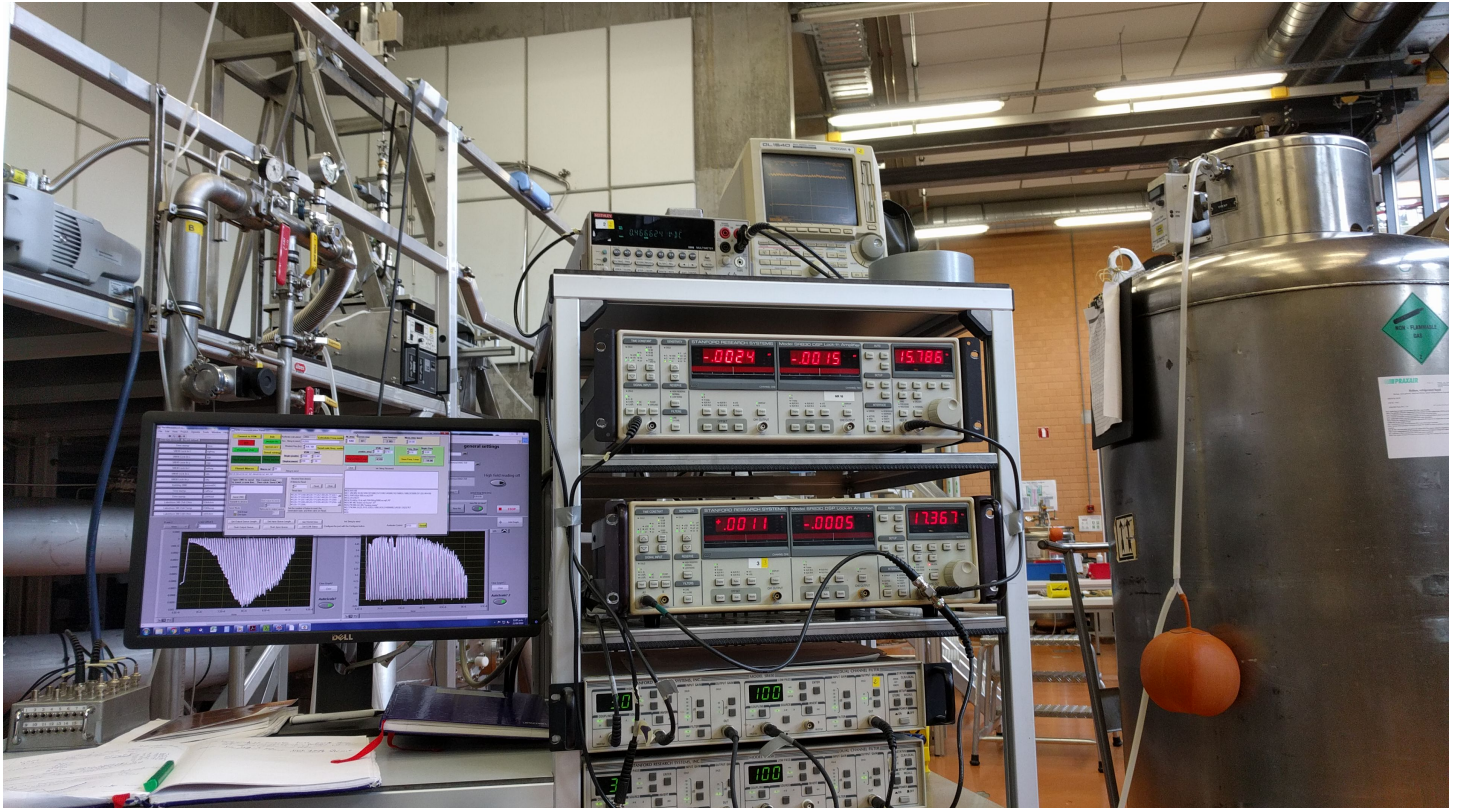


Vibrating Sample Magnetometer

High Field Magnet Laboratory

Radboud University



Andrew Ammerlaan

Supervisor: Prof. Dr. Uli Zeitler

November 30, 2018

Abstract

Vibrating sample magnetometry is a technique used to measure the magnetization of a sample. It utilizes the principle of electromagnetic induction; a magnetized sample will induce a voltage across a set of 4 pickup coils. This report contains both a in-depth analysis of the inner workings of the vibrating sample magnetometer (VSM) at HFML, and doubles as a manual for this VSM. Detailed schematics and illustrations with distance measurements are therefore included in the appendices. The VSM was used to measure the saturation magnetization of copper sulfate pentahydrate, using nickel as calibration. Furthermore the phase transition of $\text{K}\text{Er}(\text{MoO}_4)_2$ was analyzed. Finally, in collaboration with Anabel and Patrica from the University of Deusto (Bilbao, Spain) the temperature dependence of $\text{Ni}_{38}\text{Mn}_{49}\text{Sn}_9\text{Fe}_4$ and $\text{Ni}_{37}\text{Mn}_{49}\text{Sn}_9\text{Fe}_5$ was measured.

Contents

1 Theoretical principle of the VSM	3
1.1 Magnetization and Faraday's law of induction	3
1.2 The response of a pickup coil to magnetized sample	3
1.3 Flattening the curve	5
1.4 Compensating for motion of the pickup coils	5
2 Setup	7
2.1 The drive motor	7
2.2 The pickup coils	7
2.3 The potentiometer	7
3 Calibration	9
3.1 Calibrating the potentiometer	9
3.2 Centering the sample	9
3.3 Calibrating with nickel	10
4 Saturation magnetization of CuSO₄·5 H₂O	12
5 Sample holder background	14
6 Phase transition of KEr(MoO₄)₂	16
7 Phase transition in Ni₃₈Mn₄₉Sn₉Fe₄ and Ni₃₇Mn₄₉Sn₉Fe₅	18
8 Discussion	20
8.1 Different potentiometer power supplies	20
8.2 Magnetization at B is not the same as at -B?	20
8.3 Possibility for compensating for magnetization of empty sample holder	20
8.4 Different calibration parameters?	21
Acknowledgments	22
References	22
A Using the VSM motor controller program	23
B VSM measurement step-by-step	24
C Schematics and Pictures	26

1 Theoretical principle of the VSM

Materials in a magnetic field will react to this field, how they react exactly is an interesting field of study because not all materials will react in a trivial way. Some materials will exhibit phase transitions at certain magnetic field strengths, and some material's magnetization will have an interesting temperature dependence. By analyzing the magnetization of samples as a function of temperature and/or magnetic field strength, we can not only uncover interesting phenomena but also learn more about the sample material.

A vibrating sample magnetometer is capable of doing these magnetization measurements, using a set of four pickup coils. Two coils are positioned above the sample and two below. The sample is placed in a sample holder attached to a long stick. This sample stick is then screwed onto a connector piece, which in turn screws onto the top of the VSM. The length of the sample stick is adjusted such that the sample is positioned exactly between the pickup coils. The whole VSM is then inserted into a cryostat for temperature control, which in turn is inserted into a bitter magnet. This bitter magnet induces a magnetization on the sample. The connector piece on top of the VSM is attached to a motor, which sends a vibrating motion through the connector piece and causes the sample to vibrate in between the coils. The following sections explain the physical effect of the vibrating magnetized sample on a pickup coil, why 4 pickup coils are required, and why the magnetization can thus be measured accurately. Schematics and pictures of the VSM can be found in Appendix C.

1.1 Magnetization and Faraday's law of induction

Faraday's law describes the voltage that is induced in a closed loop due to a change in the magnetic field through this loop. It is given by:

$$V = -\frac{d\phi_B}{dt} \quad (1)$$

Where V is the induced voltage (also known as the 'electromotive force'), and ϕ_B is the magnetic flux through the loop which is given by:

$$\phi_B = \iint_S \vec{B}(\vec{r}, t) \cdot d\vec{A} \quad (2)$$

Where S represents the surface of the closed loop and B the magnetic field. By taking the magnetic field to be perpendicular to the surface of the closed loop, and homogeneous throughout the closed loop, Equation 2 simplifies to $\phi_B = BS$

Magnetization: The electrons in any material will react to an external magnetic field applied to this material, it will do this paramagnetically and/or diamagnetically.

Paramagnetic contributions are caused by the **magnetic moment of unpaired electrons** in the material that will align with the external magnetic field. This causes an internal magnetic field in the material which is parallel to the external field (positive magnetization).

Diamagnetism on the other hand is caused by the **Lorentz force on the electrons** causing them to circulate creating an internal magnetic field antiparallel to the external field (negative magnetization). All materials are diamagnetic to some extent, however because the electron orbitals are constrained by the Pauli principle these contributions are generally much smaller than paramagnetic contributions [5].

Once a material is magnetized it will have its own magnetic field, and will thus cause a magnetic flux through a closed loop. When the material moves with respect to the closed loop the flux will change, inducing a voltage in the closed loop. Because the induced voltage is directly related to the magnetization, it is possible to determine a sample's magnetization just by measuring the induced voltage.

1.2 The response of a pickup coil to magnetized sample

Because the inductive effect on just one closed loop is small, and because the alignment of one closed loop with respect to the magnetic field is prone to errors, a pickup coil is used instead. Since a coil is basically just a series of closed loops, we can multiply Equation 1 with N , the number of windings:

$$V(t) = -N \frac{d\phi_B}{dt} \quad (3)$$

This can be written as:

$$V(z, t) = -N \frac{d(BS)}{dz} \frac{dz}{dt} \quad (4)$$

Where S is a property of the sample proportional to its magnetization, and the z direction is parallel to the vibrating motion [4].

In an ideal situation the motion of the sample is perfectly sinusoidal, in other words $z(t) = A \cos(2\pi ft)$, and thus $\frac{dz}{dt} = -2\pi f A \sin(2\pi ft)$. If we further assume that there are no defects or other imperfections in the coil we can also use the following for its magnetic field:

$$B(z) = \frac{\mu_0 I}{2} (z - L) \left[\ln \left(r_2 + \sqrt{r_2^2 + (z - L)^2} \right) - \ln \left(r_1 + \sqrt{r_1^2 + (z - L)^2} \right) \right] + \frac{\mu_0 I}{2} z \left[\ln \left(r_1 + \sqrt{r_1^2 + z^2} \right) - \ln \left(r_2 + \sqrt{r_2^2 + z^2} \right) \right] \quad (5)$$

Where r_1 and r_2 are the inner and outer radius of the coil respectively, and L is the length of the coil [4].

Taking the derivative of Equation 5 and filling in $\frac{dz}{dt}$, we get:

$$V(z, t) = -NASI \mu_0 \pi f \sin(2\pi ft) \left[\ln \left(r_2 + \sqrt{r_2^2 + (z - L)^2} \right) - \ln \left(r_1 + \sqrt{r_1^2 + (z - L)^2} \right) + (z - L)^2 \left(\frac{1}{r_2 \sqrt{r_2^2 + (z - L)^2} + r_2^2 + (z - L)^2} - \frac{1}{r_1 \sqrt{r_1^2 + (z - L)^2} + r_1^2 + (z - L)^2} \right) + \ln \left(r_1 + \sqrt{r_1^2 + z^2} \right) - \ln \left(r_2 + \sqrt{r_2^2 + z^2} \right) + z^2 \left(\frac{1}{r_1 \sqrt{r_1^2 + z^2} + r_1^2 + z^2} - \frac{1}{r_2 \sqrt{r_2^2 + z^2} + r_2^2 + z^2} \right) \right] \quad (6)$$

From this it is immediately clear that the voltage signal from the pickup coil is also sinusoidal (90° phase shifted). In a experimental setup we will always measure the RMS value of this AC signal, therefore we take the RMS value of Equation 6:

$$V(z) = -NASI \mu_0 \frac{f\pi}{\sqrt{2}} \left[\ln \left(r_2 + \sqrt{r_2^2 + (z - L)^2} \right) - \ln \left(r_1 + \sqrt{r_1^2 + (z - L)^2} \right) + (z - L)^2 \left(\frac{1}{r_2 \sqrt{r_2^2 + (z - L)^2} + r_2^2 + (z - L)^2} - \frac{1}{r_1 \sqrt{r_1^2 + (z - L)^2} + r_1^2 + (z - L)^2} \right) + \ln \left(r_1 + \sqrt{r_1^2 + z^2} \right) - \ln \left(r_2 + \sqrt{r_2^2 + z^2} \right) + z^2 \left(\frac{1}{r_1 \sqrt{r_1^2 + z^2} + r_1^2 + z^2} - \frac{1}{r_2 \sqrt{r_2^2 + z^2} + r_2^2 + z^2} \right) \right] \quad (7)$$

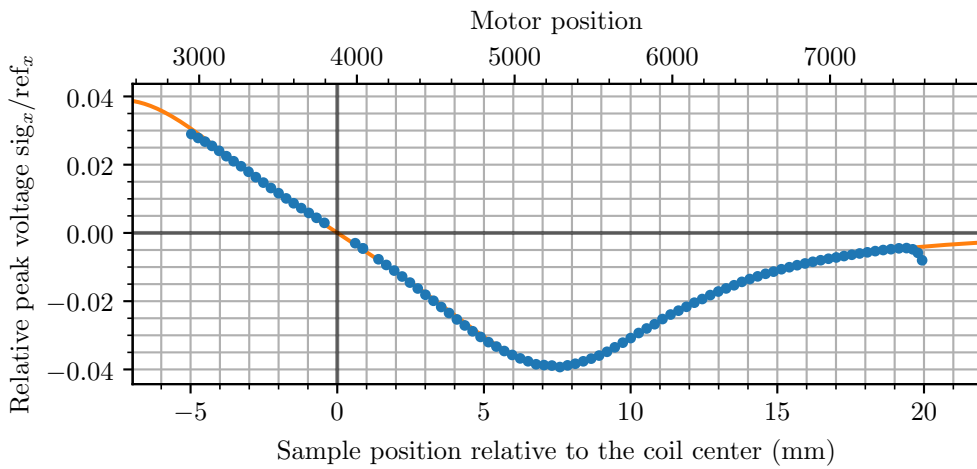


Figure 1: The response of one of the pickup coils (upper large, designated '1-2' in Appendix C on page 29) to the vibrational motion (18.1 Hz, 1.08 mm) of a permanent magnet with a mass of 30.9 mg as a function of the position. Note that the coordinates on the lower axis have been shifted such that 0 responds to the coil center. The theoretical curve has been fitted through the data, Equation 7.

We can check if this equation holds by making a plot of the response of 1 pickup coil as a function of

the position at which the sample is vibrating (z), and fitting Equation 7 through this data, as shown in Figure 1.

1.3 Flattening the curve

The attentive reader will notice 2 things in Figure 1. First, the quantity on the y-axis: This is actually not $V(z)$ as in Equation 7 but $V(z)$ divided by a reference voltage that is directly proportional to the vibrating motion of the VSM's motor. The reason for this will be discussed in more detail in Section 2.3. Second, the plot in Figure 1 is not flat anywhere, which is a problem because this means that the sample will induce a different response throughout its vibrating motion. Because of this the signal is not going to be a perfect sine, since the signal will be higher closer to the coil and lower further away. For an accurate measurement we want a nice sine wave as VSM signal, thus we need a flat area in the plot that is at least as big as twice the amplitude of the sample's motion.

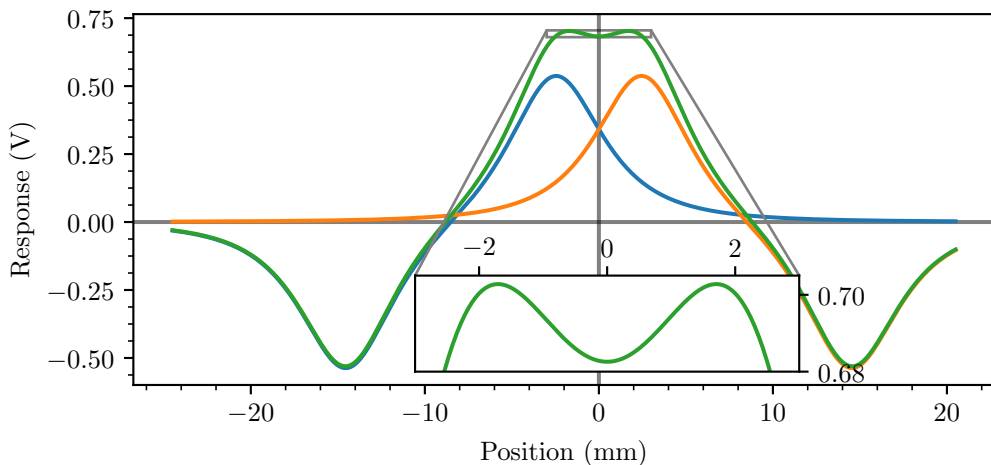


Figure 2: The superposition of the response of 2 coils, separated by a distance of 5 mm. Where the blue and orange curve represent the different coils, and the coils are connected such that the bottom of both coils are connected to each other. Because both coils are on opposite sides of the sample, this will cause both coils to respond with the same sign. In other words, one of the graphs is mirrored in the z-axis such that both peaks superimpose (green curve). Creating a approximately flat area on the peak of the superposition of both coils. For demonstration purposes the separation between the coils has been increased to 5 mm, the actual separation is 2.5 mm. Figure 3 contains the equivalent of the green curve with actual data points, but for a shorter z-axis range.

This can be accomplished by measuring the combined responses of several pickup coils instead of just one. When a second coil is added on the other side of the sample and connected such that it responds oppositely (its response curve (Figure 1) is mirrored in the z-axis) the peaks of both coil start to merge, as demonstrated in Figure 2. By carefully choosing the separation between these 2 coils, we get a nice and flat (0.1% deviation [4]) area, as shown in Figure 3. (This is actually the combined response of not 2 but 4 pickup coils, see also Section 1.4)

1.4 Compensating for motion of the pickup coils

It is impossible to keep the VSM completely still inside the bitter magnet. There will always be unwanted vibrations caused by the various pumps, motors or water currents throughout the lab. These unwanted vibrations cause the pickup coils themselves to move inside the external magnetic field. While this field is quite homogeneous (1×10^{-3} cm DSV in cell 3 [2]) any such movement results in a small magnetic flux that will result in noise on the signal. A solution is to add an oppositely wound twin coil inside both pickup coils. This can compensate for any movements inside the external magnetic field, since these unwanted vibration will cause both this compensation coil and its parent coil to move in exactly the same way. For this compensation coil to cancel out these external vibrations the flux has to be exactly opposite to the flux that these vibrations cause in the parent coil. To accomplish this the compensating

coil has to have a smaller radius, and thus needs to have a larger number of windings, such that the surface area of one winding multiplied by the number of windings is equal. When the flux through both coils cancel each other out completely, there will be no overall effect of external vibrations on the signal when measuring across the combination of all coils.

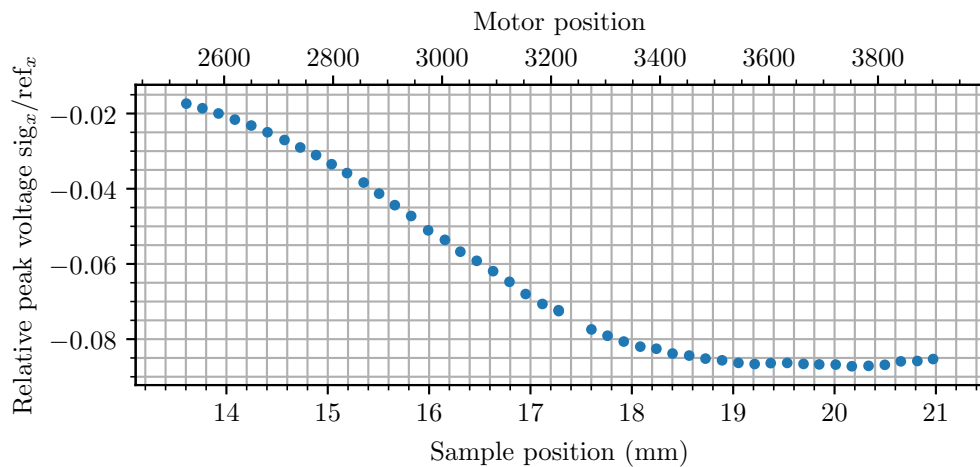


Figure 3: The response of the combination of all four pickup coils (designated '9-10' in Appendix C on page 29) to the vibrational motion (18.1 Hz, 1.08 mm) of a nickel sample with a mass of 42.5 mg as a function of the position. The magnetization has been induced on the sample by an external magnetic field of 2 T in cell 3. The numbers on the lower axis are converted from the ones on the upper axis, this axis has its 0 when the motor driving the VSM is in the all the way up position.

Note that Figure 3 covers a shorter z-axis range than Figure 1, due to restrictions in the movement of the motor driving the VSM (more on this in the Section 2.1 and Section 2.3). If we were to continue the measurement beyond 21 mm, it will of course approximately follow the curve in Figure 2 and return to zero.

2 Setup

The whole VSM setup consists of 3 major components: the motor, the pickup coils and a potentiometer. This section will look into each component, and additional equipment needed to correctly analyze and record data from each component. A detailed schematic of the VSM setup can be found in Appendix C on page 29

2.1 The drive motor

The samples motion is driven by an electric motor, which is in turn controlled by a motor controller (LAC-25, Figure 22). This motor controller can receive commands from a computer using a VSM control program written by Hung van Luong. In this control program the user sets the desired amplitude and starting position, after which the computer will send the necessary commands to the motor. More detailed instructions on how to use this program can be found in Appendix A.

However if the motor were to be connected directly to the sample stick, the pumping up/down motion of the stick will cause undesired pressure changes inside the VSM. Therefore the motor does not drive the sample's motion directly instead it drives a connector piece on top of the VSM (Figure 21a). This connector piece seals the inside of the VSM and therefore prevents any pressure changes. The connector piece then passes on the vibrating motion of the motor to the sample stick (Figure 21b).

2.2 The pickup coils

When a sample is set to vibrate such that the sample is within the flat area (in Figure 3), we get a sinusoidal VSM signal from the combination of all 4 pickup coils, the frequency of which should be the same as the frequency of the sample's vibration. Previous research [3] has determined that a frequency of 18.1 Hz causes least noise in the VSM's signal, so this will be the frequency we will send to the motor. The VSM signal first goes through a Stanford Research 650 Dual-Channel filter, set to filter out everything below 4 Hz and above 80 Hz. Furthermore the filter also amplifies the signal, the amplification required depends on the amplitude of the original signal, and thus on the magnetization. The signal is then sent through a Stanford Research 830 Lock-In amplifier, which measures both the real and imaginary components of the signal and send these back to the computer. The signal can also be monitored visually on a oscilloscope, using the 'monitor out' of the lock-in. This is useful, because it enables us to check if the signal is truly sinusoidal and allows us to choose the correct amplification.

2.3 The potentiometer

Because of friction, the actual motion of the motor is not necessarily equal to what was set by the user on the computer. This would not be a big problem if the friction were to be the same at each motor position. However there is a position dependent component to this friction, caused by the (springs of the) connector piece whose friction depends strongly on how much the spring is compressed (Section 2.1 and Figure 21a). As a result the amplitude when vibrating in a position that leaves the connector piece's springs more or less in their rest position will be significantly larger than when the connector piece's springs are pushed all the way down or up. Furthermore, for high external magnetic fields the sample is going to be attracted to the center of the bitter magnet, thus reducing the amplitude even further. This reduction in amplitude is directly visible in the VMS's signal (right part of Figure 5), which might lead one to conclude that the magnetization has decreased, when in fact it has not.

To record the actual motion of the motor (and thus the sample) we connect a potentiometer (Honeywell SLF01N1500B6A) to the motor. The potentiometer will return a certain fraction of a voltage applied to it depending on the position of the motor (and thus the sample). When the motor starts vibrating this fraction will change accordingly, thus creating a AC (vibration) signal on top of a DC (position) signal.

To supply the potentiometer with power, I have made a box (Figure 4, and Appendix C on page 29) that uses 2 AA batteries to create a 3 V voltage across the potentiometer. The box will separate both the AC and DC components from the signal returned by the potentiometer. The DC component is then sent to a Agilent 34410 multimeter, which sends it back to the computer. The AC component is sent through a Stanford Research 650 Dual-Channel filter and Stanford Research 830 Lock-In amplifier first, after which it can be recorded on the computer and displayed on the oscilloscope as well.

Because the battery depletes over time, we record the current battery voltage on a Keithley 2000 multimeter. Dividing the AC and DC components by this voltage then makes the AC and DC signals

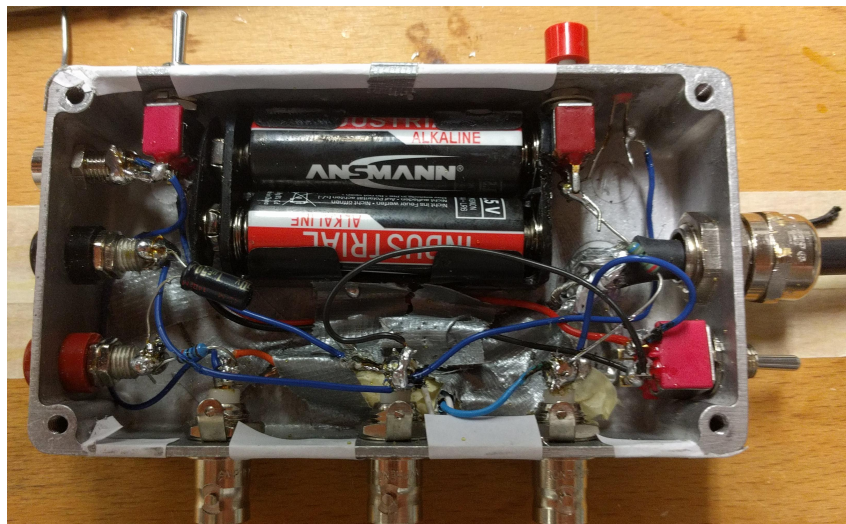


Figure 4: The box that supplies the potentiometer with power (2x1.5 V), and outputs the AC and DC component of the returned signal.

dimensionless and compensates for battery drain. We can then use the potentiometer as a reference by dividing the VSM's signal by the potentiometer's signal. Because both signals will reflect the changed amplitude in the same way, dividing them like this cancels out the reduction in amplitude, thus eliminating the effects of the position dependent friction, as has been done in Figure 1 and Figure 3.

3 Calibration

Now the sample motion can be controlled, and the response signal from the pickup coils and the potentiometer can be measured. However, before any measurement can be done, the VSM first needs to be calibrated. First the potentiometer's DC component must be calibrated, in order to know the position of the sample at any given time. Next we need to find the position that leaves the sample exactly between the pickup coils, the flat area in a position loop plot. And finally the VSM's signal has to be calibrated with a sample of known magnetization.

3.1 Calibrating the potentiometer

To calibrate the potentiometer's DC component, simply set the VSM to vibrate at some position and read off the DC voltage on a multimeter or the computer. Do this for say 4 to 5 points, and make a linear fit through these points, this will yield parameters 'a' and 'b' ($position = a* voltage_{DC} + b$). These parameters will be used in the next section, to convert the recorded DC component back to a position and plot the VSM's signal as a function of this position (Figure 3). Note that this calibration needs to be redone every time the sample changes or the motor/connector piece/potentiometer is adjusted, because there is no way the (new) sample is going to be in exactly the same position after any adjustments.

3.2 Centering the sample

Next we must make sure that the tip of the VSM (coils + sample) is approximately in the center of the external magnetic field. This can be done by using the given specifications of the magnet [2], and the known lengths of the VSM parts (as found in Appendix C). The VSM can be moved up/down as needed with the screw shown in Figure 20. Furthermore to get a nice sinusoidal signal from the VSM it is even more important that the sample is set to vibrate exactly between the upper and lower pickup coils (the flat area in Figure 3). To accomplish this we need to measure the VSM signal as a function of the sample's position. For this purpose the VSM's control program has a 'position loop' option. This will set the VSM to vibrate at a set begin position for a set amount of time. After which it will move a set distance down, and vibrate for that same amount of time at that position, and so on.

When analyzing the VSM's signal on the lock-in we will see that most of the signal is imaginary since the coils impedance is mostly inductive. We can use the lock-in's "autophase" function to phase shift the signal such that almost all of the signal is real. We can then use the real part in our response versus position plots, since any change in the imaginary part is just noise.

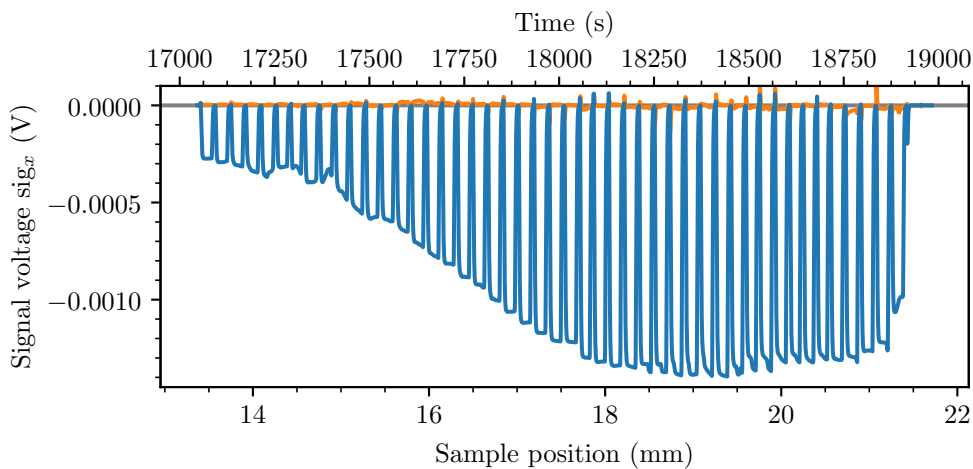


Figure 5: The response of the combination of four pickup coils (designated '9-10' in Appendix C on page 29) to the vibrational motion (18.1 Hz, 1.08 mm) of a nickel sample with a mass of 42.5 mg as a function of the position. The magnetization has been induced on the sample by an external magnetic field of 2 T in cell 3. This figure contains the unprocessed data used to create Figure 3. The blue curve is the real part, while the orange curve represents the imaginary part.

Doing such a position loop for nickel will yield a graph as shown in Figure 5. In this figure we see that the resistive part (imaginary after “autophase”) will fluctuate a bit as well. We can ignore this because we are only interested in the inductive part when looking for the flat area.

If we then divide Figure 5 by the reference we get Figure 6. The advantage of dividing by the reference is immediately clear: Not only does the curve look smoother, it also compensates for the reduced amplitude of the VSM’s motor (Section 2.3). This is particularly visible in the right of the plot, where in Figure 5 there is a significant reduction in amplitude. That is not visible at all in Figure 6.

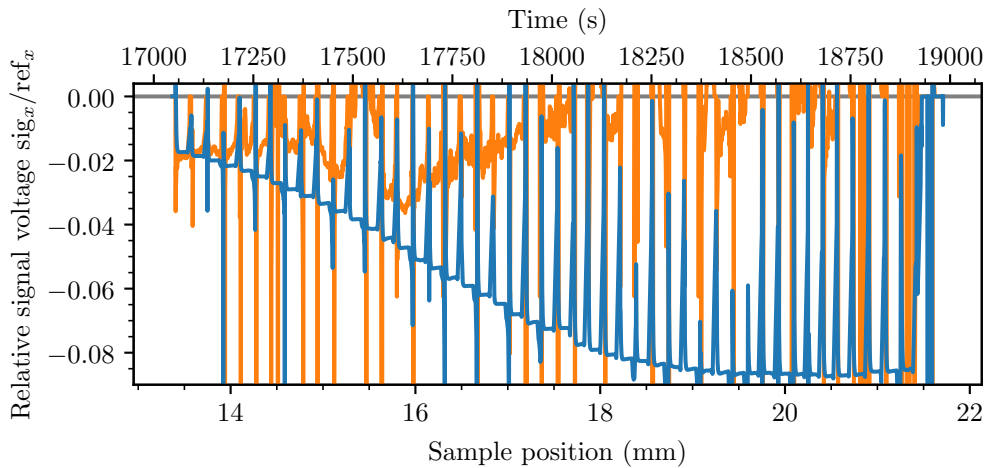


Figure 6: The response of the combination of four pickup coils (designated ‘9-10’ in Appendix C on page 29) to the vibrational motion (18.1 Hz, 1.08 mm) of a nickel sample with a mass of 42.5 mg as a function of the position. The magnetization has been induced on the sample by an external magnetic field of 2 T in cell 3. This figure is Figure 5 divided by the reference. The blue curve is the real part, while the orange curve represents the imaginary part.

However there is also a disadvantage to dividing by the reference, demonstrated by the spikes in Figure 6. These spikes are caused by points where the reference becomes almost 0 for a brief time, dividing by these near-zero numbers will cause very large positive or negative points in the plot. This is unavoidable since the motor has to stop before it can move to the next position. However, if we identify where each peak occurs in the data file before dividing by the reference, and use only those points after the division, we circumvent the divide-by-zero problem.

To automate this process I have made a simple python script, which can be found here [1]. Which takes data from any raw data file (e.g. Figure 5), locates each peak, divides by the reference, and then calculates the average and standard deviation of each peak. It then takes these data points and plots them against the position, converted from the DC component of the potentiometer’s signal, and if able fits Equation 7 through the data (Figure 1 and Figure 3). More detailed instructions on how to use this can be found in the script’s readme file, and on github [1]. Now that we have such a plot, we can easily identify the flat area and choose the sample’s vibration position accordingly.

3.3 Calibrating with nickel

To measure the unknown magnetization of a sample, we must first calibrate the VSM’s signal using a sample with a known magnetization, such as nickel. The saturation magnetization of nickel has been measured to be (58.57 ± 0.03) emu/g [6]. Therefore our sample (42.5 mg) should have a magnetization of (2.489 ± 0.002) emu

By setting the VSM to vibrate within the flat area and changing the strength of the external magnetic field, we obtain a plot as in Figure 7. Here we can see that nickel saturates at about 1 T, we can now calculate the average and standard deviation of all points from the saturation point onwards. We find that our saturated nickel sample ((2.489 ± 0.002) emu) gives an absolute relative signal of 0.0848 ± 0.0002 . Now using the fact that 0 magnetization should give 0 signal, we can make a linear fit. Which gives a calibration constant of $c = (29.34 \pm 0.06)$ emu (*magnetization = c * signal*)

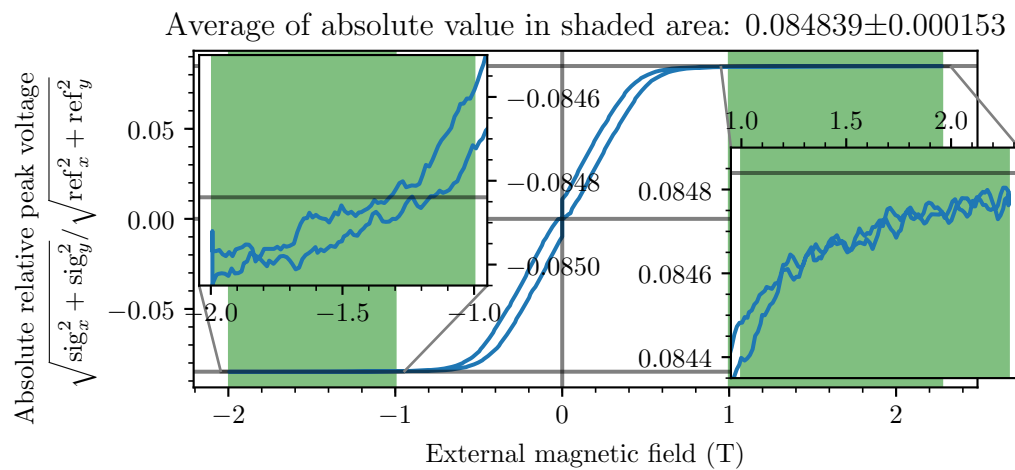


Figure 7: The response of the combination of four pickup coils (designated '9-10' in Appendix C on page 29) to the vibrational motion (18.1 Hz, 1.08 mm) of a nickel sample with a mass of 42.5 mg. As a function of the applied external magnetic field in cell 3, at room temperature. The rate of change in the field was 20 mT s^{-1} , and the amplification on the signal and reference were both set to 30 dB.

4 Saturation magnetization of $\text{CuSO}_4 \cdot 5 \text{H}_2\text{O}$

Now that we have calibrated the VSM, we can measure the unknown magnetization of any sample, such as copper sulfate pentahydrate. This sample has a very small magnetization, since it consists mostly of diamagnetic atoms, thus enabling us to test how sensitive the VSM is. In fact, at room temperature the magnetization of this material is so small, that it is near impossible to distinguish from an empty sample holder (Figure 8). Besides, at room temperature copper sulfate will not saturate within the range of the cell 3 bitter magnet (max 33 T).

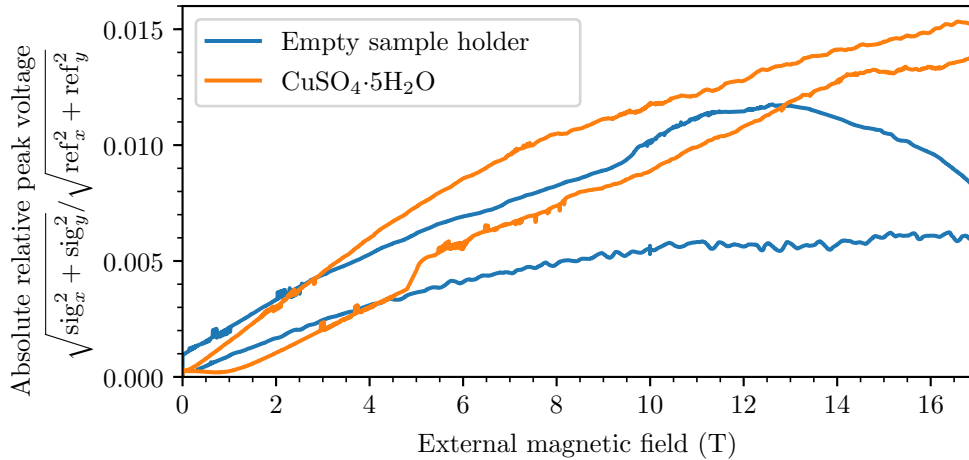


Figure 8: The response of the combination of four pickup coils (designated '9-10' in Appendix C on page 29) to the vibrational motion (18.1 Hz, 1.08 mm) of a $\text{CuSO}_4 \cdot 5 \text{H}_2\text{O}$ sample with a mass of 143 mg. As a function of the applied external magnetic field in cell 3, at room temperature. Compared to the same experiment with an empty sample holder.

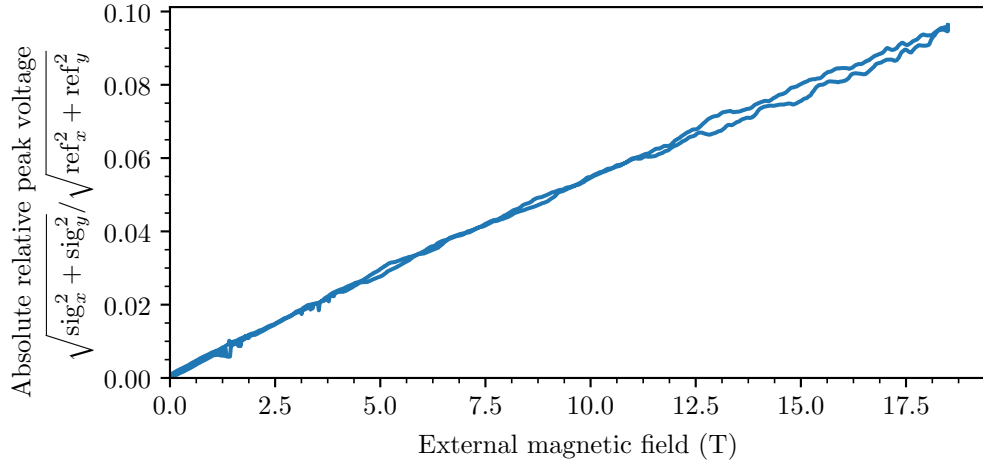


Figure 9: The response of the combination of four pickup coils (designated '9-10' in Appendix C on page 29) to the vibrational motion (18.1 Hz, 1.08 mm) of a $\text{CuSO}_4 \cdot 5 \text{H}_2\text{O}$ sample with a mass of 143 mg. As a function of the applied external magnetic field in cell 3, at 15 K. The rate of change in the field was 10 mT s^{-1} , and the amplification on the signal and reference were 40 dB and 20 dB respectively.

To measure the saturation magnetization anyway, we need to cool the sample down using cryostat 2 [2]. Because at low temperatures it is easier to induce magnetization, since there is less randomization of the direction of the magnetic moments due to thermal energy. The cryostat's thermometers (46682) and heater as well as the VSM's internal thermometer (x07377) are connected to a LakeShore 350 which controls the cryostat and measures the temperature in the cryostat and the VSM. In Figure 9

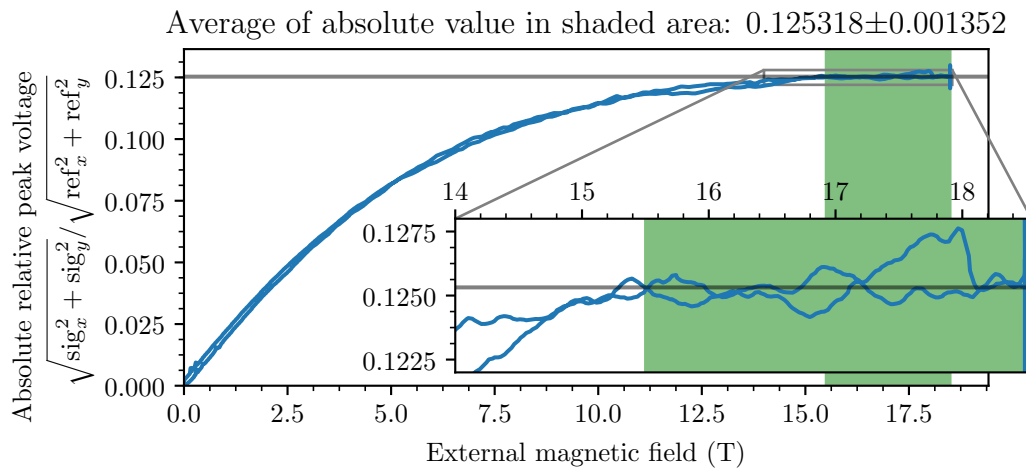


Figure 10: The response of the combination of four pickup coils (designated '9-10' in Appendix C on page 29) to the vibrational motion (18.1 Hz, 1.08 mm) of a $\text{CuSO}_4 \cdot 5 \text{H}_2\text{O}$ sample with a mass of 143 mg. As a function of the applied external magnetic field in cell 3, at 4 K. The rate of change in the field was 10 mT s^{-1} , and the amplification on the signal and reference were 40 dB and 20 dB respectively. The reference has been corrected to correspond to the reference used in Figure 7, using the slopes of the potentiometer calibration.

we see that copper sulfate does not yet saturate at 15 K, thus we need to go down further to 4 K (Figure 10) where saturation occurs at about 15.5 T. The calibration of the potentiometer was very different between the nickel and copper sulfate measurements ($y = 4287.347911 * x + 736.918625$ compared to $y = 8830.788615 * x + 238.4372817$, see section 8). This means that if we divide each measurement by their respective reference we cannot do a direct comparison between the two. However, since the calibration parameters for both measurements are known, we can easily compensate for this by using the ratio of the slopes (a_1/a_2) of both calibrations: After also compensating for amplification on the VSM's signal by the filter we can now divide the signal by the corrected reference and plot this (Figure 10). We see that at saturation we get a relative absolute signal of 0.125 ± 0.002 . Using the calibration parameter 'c' obtained in Section 3.3 we obtain a saturation magnetization of (3.67 ± 0.04) emu, which gives (25.7 ± 0.3) emu/g.

Sanity Check: In copper sulfate pentahydrate most of the magnetization is due to the Cu^{++} ions. These ions, being a spin $1/2$ system, have a spin magnetic moment of $2\sqrt{s(s+1)} = \sqrt{3} \mu_B$. Using the atomic mass given in table 1, we get a magnetization of 39 emu/g. Which is the same order of magnitude as the measured magnetization, they are however not equal. This is because we have only taken into account the magnetization of the copper ions, however the sulfate ions and water molecules will also have some diamagnetic contribution lowering the overall magnetization.

Element	Atomic mass (u)
Cu	63.546
S	32.065
9 O	9×15.9994
10 H	10×1.00794
$\text{CuSO}_4 \cdot 5 \text{H}_2\text{O}$	249.684

Table 1

5 Sample holder background

To further analyze the sensitivity of the VSM we measure the VSM's response to an empty sample holder and compare it to 1.2 mg of nickel, as shown in Figure 11.

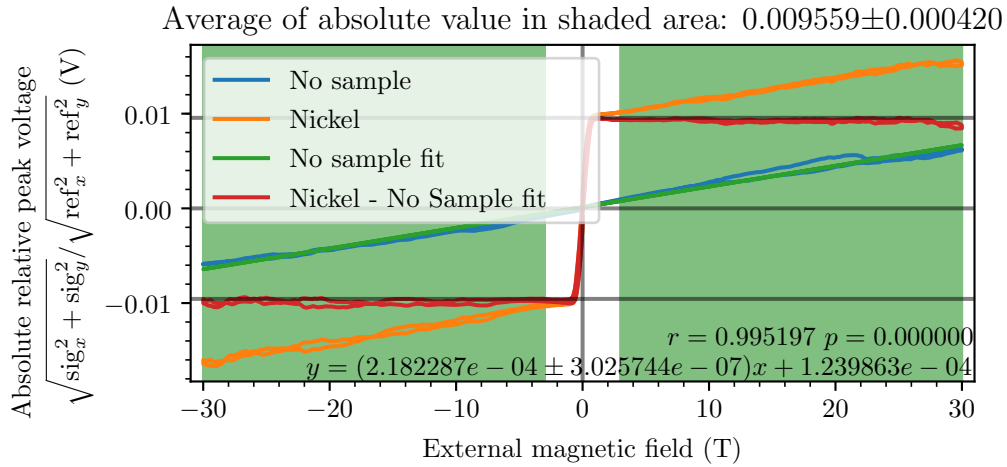


Figure 11: The response of the combination of four pickup coils (designated '9-10' in Appendix C on page 29) to the vibrational motion (18.1 Hz, 2.40 mm) of a nickel sample with a mass of 1.2 mg and an empty sample holder. As a function of the applied external magnetic field in cell 5, at room temperature. The rate of change in the field was 33.33 mT s^{-1} , and the amplification on the signal and reference were 40 dB and 0 dB respectively. The reference has been corrected by dividing it by the battery voltage, making the reference dimensionless.

It is clear that the empty sample holder has a linear response within the range of the bitter magnets, when subtracting a linear fit of this background from the nickel curve it becomes flat, as it should be. Figure 11 shows the response of the sample holders used in all previous measurements, however a new type of sample holder (Figure 12) has been developed using a 3D-printer. It is hexagonal and therefore has superior helium flow along its six sides compared to the circular sample holder. Its response is shown in Figure 13 (room temperature) and Figure 14 (190 K).

Note that during the measurements in Figure 13 and Figure 14 the potentiometer had reached the end of its lifetime. The wiper kept losing contact which caused significant noise in the reference signal, which increased over time. This caused the lock-in to register a decreasing reference time, making the reference signal unusable as a reference. To get a correct order of magnitude in the plot while preserving the shape, the signal in Figure 13 has been divided by a constant instead. This constant was chosen such that the average of points beyond saturation is the same in Figure 13 and Figure 11. However this means that Figure 13 and Figure 14 are correct in shape only, the numbers in these figures are educated guesses only. That being said, it is still clear that the slope from the new sample holder is smaller than that of the old sample holder. Thus the new sample holder has slightly smaller background noise. Furthermore, from Figure 14 we can conclude that the temperature dependence of this background noise is negligible. Following these measurements the potentiometer was replaced with a spare one of the same model.

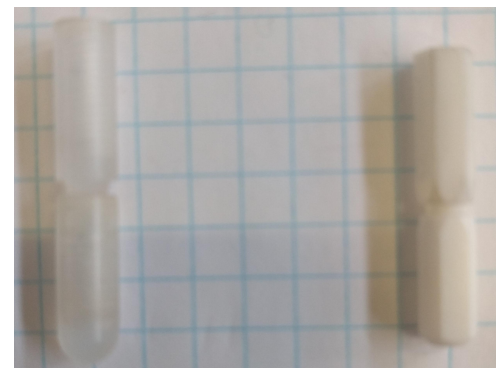


Figure 12: Old sample holder (left) and new sample holder (right).

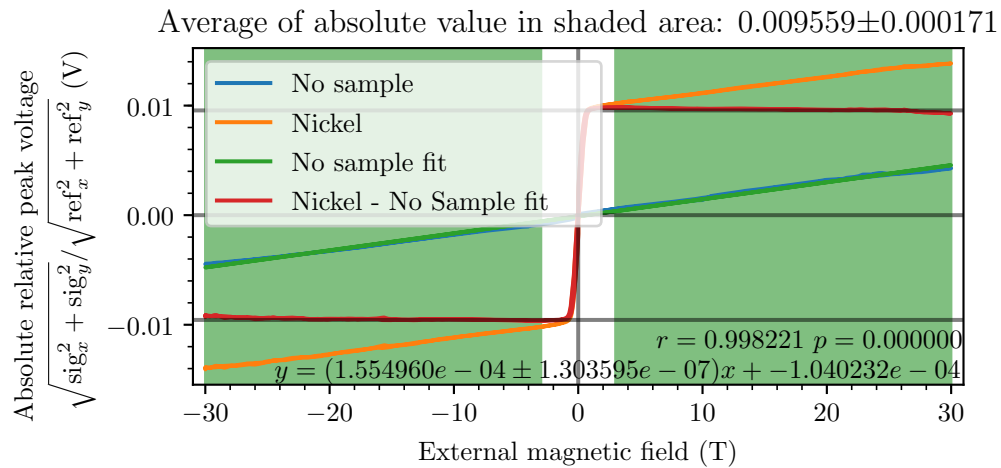


Figure 13: The response of the combination of four pickup coils (designated '9-10' in Appendix C on page 29) to the vibrational motion (18.1 Hz, 2.40 mm) of a nickel sample with a mass of 1.2 mg and an empty sample holder (new version). As a function of the applied external magnetic field in cell 5, at room temperature. The rate of change in the field was 33.33 mT s^{-1} , and the amplification on the signal and reference were 40 dB and 0 dB respectively. The reference has been corrected by dividing it by the battery voltage, making the reference dimensionless.

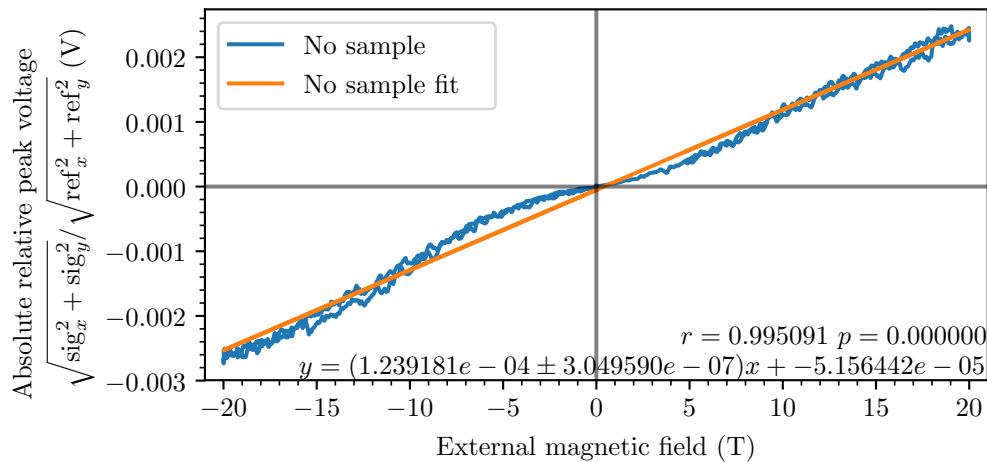


Figure 14: The response of the combination of four pickup coils (designated '9-10' in Appendix C on page 29) to the vibrational motion (18.1 Hz, 2.40 mm) of an empty sample holder (new version). As a function of the applied external magnetic field in cell 5, at 190 K. The rate of change in the field was 33.33 mT s^{-1} , and the amplification on the signal and reference were 40 dB and 0 dB respectively. The reference has been corrected by dividing it by the battery voltage, making the reference dimensionless.

6 Phase transition of KER(MoO₄)₂

Now that we have successfully found the saturation magnetization of CuSO₄·5 H₂O and have measured the background signal from the empty sample holder(s). We can measure the magnetization of a more interesting sample: KER(MoO₄)₂, which has a magnetic phase transition at around 20 T. The sample was provided by dr. Dmytro Kamenskyi and Bence Bernáth, who were researching this material. First we again measure the background for this specific sample holder, because the data in Figure 13 and 14 is not reliable (see Section 5) The background level as a function of magnetic field can be obtained directly from a nickel calibration. Since nickel's magnetization does not change after saturation any change in signal beyond the saturation point has to be background noise.

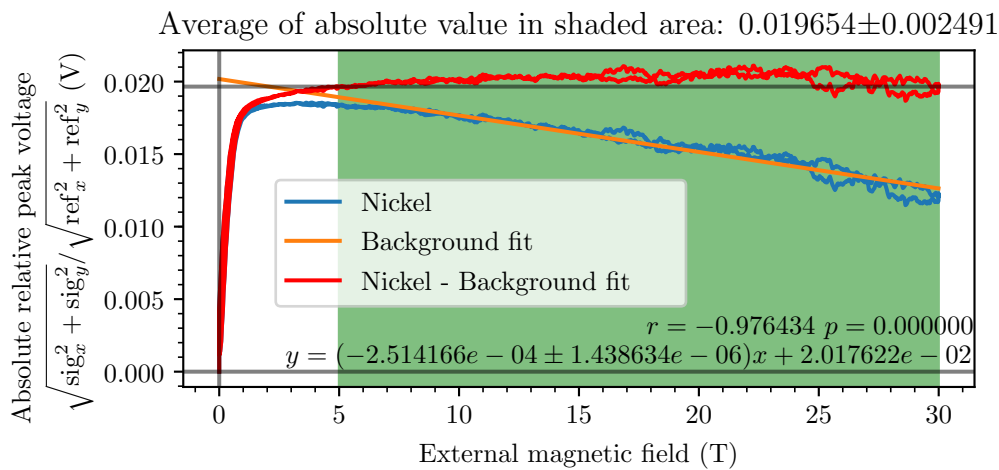


Figure 15: The response of the combination of four pickup coils (designated '9-10' in Appendix C on page 29) to the vibrational motion (18.1 Hz, 2.40 mm) of a nickel sample with a mass of 1.2 mg (new sample holder). As a function of the applied external magnetic field in cell 5, at 1.3 K. The rate of change in the field was 66.67 mT s⁻¹, and the amplification on the signal and reference were 40 dB and 0 dB respectively. The reference has been corrected by dividing it by the battery voltage, making the reference dimensionless.

In Figure 15 the response of a small nickel sample in a new sample holder is shown. A line is fitted through the data from 5 T to 30 T, this fit is then used as background level. The red curve shows the data after subtracting the slope of the fit times the magnetic field. Using the magnetization and mass of the sample ((58.57 ± 0.03) emu/g [6] and 1.2 mg) and the average signal at saturation ((0.020 ± 0.003) V), we obtain a calibration parameter of $c = (3.6 \pm 0.2)$ emu/V. Note that the unit of the calibration parameter differs from the one in Section 3.3 because for these measurements the box (Figure 4) was used. This means that the reference has been made dimensionless by dividing by the battery voltage and that thus the signal now has the unit Volt.

Figure 16 shows the response of KER(MoO₄)₂, the magnetization has been plotted on the secondary axis using the calibration parameter obtained from Figure 15. The phase transition is clearly visible somewhere between 15 T and 20 T. We also see that the curve becomes sharper as the temperature decreases. This is because as the temperature decreases less electrons will leave the groundstate, and therefore less electrons will jump between the two states as the energy levels shift closer together due to the magnetic field.

The 2.4 K curve shows a lot of hysteresis at high magnetic fields, this is caused by an experimental problem called the 'Helium bubble issue'. When the magnetic field is high diamagnetic repulsion will push helium gas to the field center, this causes helium gas to accumulate in the middle of the magnet. Which locally reduces the thermal isolation, and thus increases the temperature slightly and reduces the magnetization. The helium bubble issue is not present in the 1.3 K curve because at this temperature helium is superfluid and thus has very high thermal conductivity and therefore no bubbles.

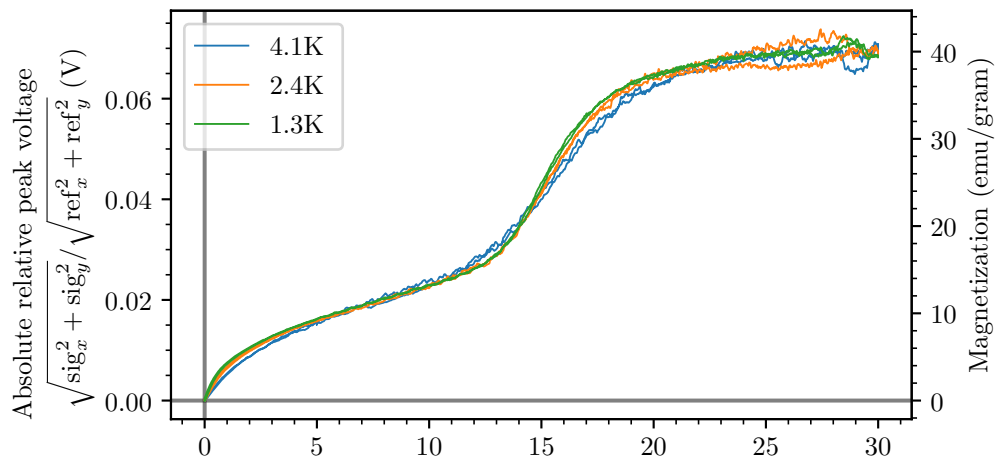


Figure 16: The response of the combination of four pickup coils (designated '9-10' in Appendix C on page 29) to the vibrational motion (18.1 Hz, 2.40 mm) of a KEr(MoO₄)₂ sample with a mass of 6.2 mg (new sample holder). As a function of the applied external magnetic field in cell 5, at different temperatures. The rate of change in the field was 33.33 mT s⁻¹, and the amplification on the signal and reference were 40 dB and 0 dB respectively. The reference has been corrected by dividing it by the battery voltage, making the reference dimensionless. The background signal obtained from Figure 15 has been subtracted from the data.

7 Phase transition in $\text{Ni}_{38}\text{Mn}_{49}\text{Sn}_9\text{Fe}_4$ and $\text{Ni}_{37}\text{Mn}_{49}\text{Sn}_9\text{Fe}_5$

The following section shortly describes the research of Anabel and Patricia from the University of Deusto (Bilbao, Spain) using the VSM at HFML, more information on this will be available in their paper. The materials $\text{Ni}_{38}\text{Mn}_{49}\text{Sn}_9\text{Fe}_4$ and $\text{Ni}_{37}\text{Mn}_{49}\text{Sn}_9\text{Fe}_5$ are Heusler alloys, and they exhibit a phase transition from a austenite phase (face-centered cubic) to a martensite phase (strained body-centered tetragonal). Before measuring these samples though, we first do another nickel calibration.

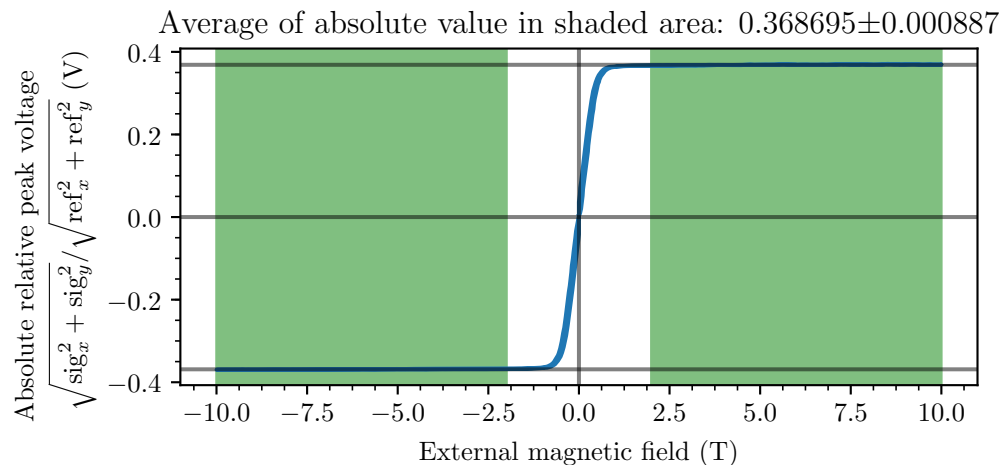


Figure 17: The response of the combination of four pickup coils (designated '9-10' in Appendix C on page 29) to the vibrational motion (18.1 Hz, 2.40 mm) of a nickel sample with a mass of 49.5 mg (new sample holder). As a function of the applied external magnetic field in cell 5, at 100 K. The rate of change in the field was 33.33 mT s^{-1} , and the amplification on the signal and reference were 10 dB and 0 dB respectively. The reference has been corrected by dividing it by the battery voltage, making the reference dimensionless.

Using the magnetization and mass of the sample ($(58.57 \pm 0.03) \text{ emu/g}$ [6] and 49.5 mg) and the average signal at saturation ($(0.3687 \pm 0.0009) \text{ V}$), we obtain the calibration parameter $c = (7.8635 \pm 0.0004) \text{ emu/V}$. This calibration parameter is used in Figure 18 and 19 to calculate the magnetization. Note that this calibration parameter is about twice that of the calibration parameter in the previous section, this is explained in Section 8.4.

The first sample's ($\text{Ni}_{38}\text{Mn}_{49}\text{Sn}_9\text{Fe}_4$) response is plotted in Figure 18. The phase transition shows a strong temperature dependence, as the temperature decreases the phase transition is stretched out. This makes sense because a smaller temperature means less movement of the atoms, thus the structural rearrangement associated with this phase transition is slower.

The second sample $\text{Ni}_{37}\text{Mn}_{49}\text{Sn}_9\text{Fe}_5$ has one nickel less and one iron more. It's phase transition (Figure 19) shows less temperature dependence. However the interesting thing in this sample is that the phase transition point depends on the sample's history. There is a difference between first cooling the sample then sweeping the field up and down, and first sweeping up, cooling down and then sweeping down (field cooling). This is seen by comparing the 'field cooling' and non 'field cooling' lines at the same temperature. For small magnetic fields the curves are similar, however at high fields the magnetization is lower for the 'field cooling' curves.

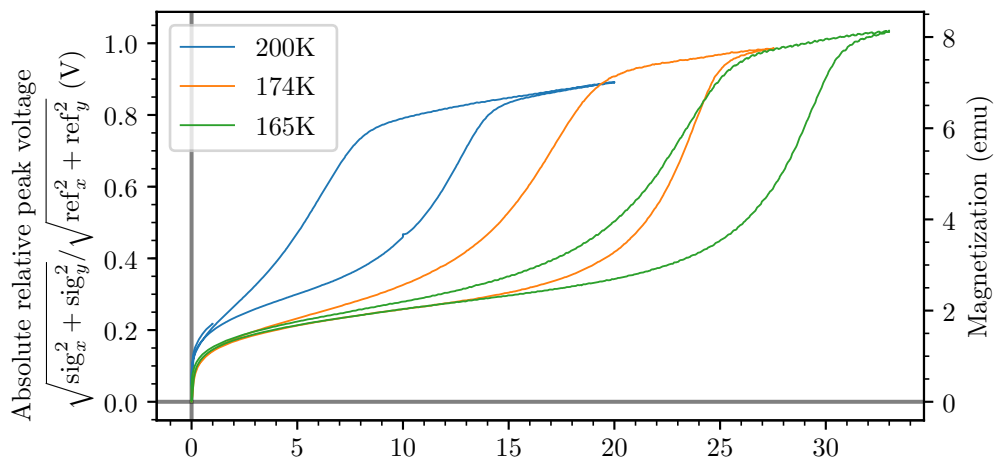


Figure 18: The response of the combination of four pickup coils (designated '9-10' in Appendix C on page 29) to the vibrational motion (18.1 Hz, 2.40 mm) of a $\text{Ni}_{38}\text{Mn}_{49}\text{Sn}_9\text{Fe}_4$ sample (new sample holder). As a function of the applied external magnetic field in cell 5, at different temperatures. The rate of change in the field was 33.33 mT s^{-1} , and the amplification on the signal and reference were 10 dB and 0 dB respectively. The reference has been corrected by dividing it by the battery voltage, making the reference dimensionless. The background signal obtained from Figure 15 has been subtracted from the data.

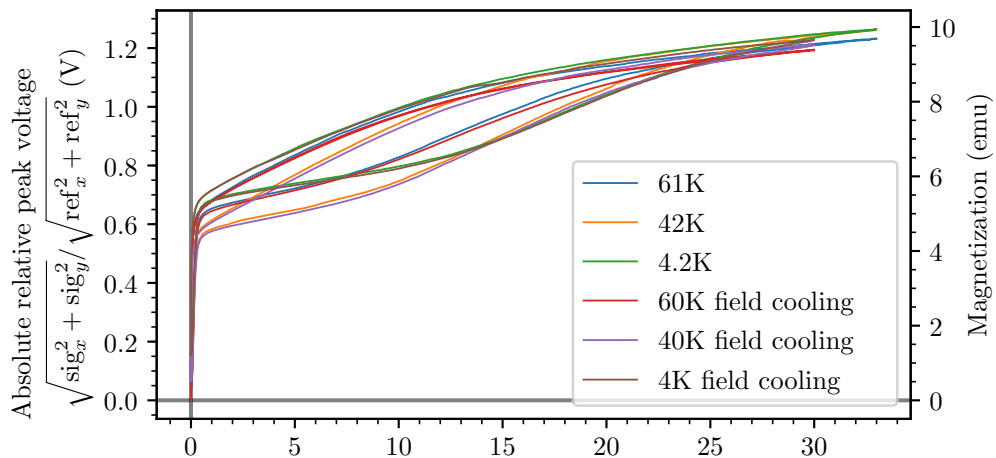


Figure 19: The response of the combination of four pickup coils (designated '9-10' in Appendix C on page 29) to the vibrational motion (18.1 Hz, 2.40 mm) of a $\text{Ni}_{37}\text{Mn}_{49}\text{Sn}_9\text{Fe}_5$ sample (new sample holder). As a function of the applied external magnetic field in cell 5, at different temperatures. The rate of change in the field was 66.67 mT s^{-1} , and the amplification on the signal and reference were 10 dB and 0 dB respectively. The reference has been corrected by dividing it by the battery voltage, making the reference dimensionless. The background signal obtained from Figure 15 has been subtracted from the data.

8 Discussion

8.1 Different potentiometer power supplies

The large difference in potentiometer calibration in Section 4 arises from the fact that we have used different power supplies for the potentiometer throughout the duration of this report. Initially a Keithley 236 current source was used. However, this (very expensive) piece of equipment is a complete overkill for the purpose of supplying a voltage to a potentiometer. Therefore the plan was to make a box (Figure 4) that will supply this voltage, and which also includes a 1 Hz filter to separate the DC component.

We first tested the feasibility of this by using a simpler voltage source (Delta elektronika power supply E015-2), which was used during the copper sulfate experiments. However the voltage on this source was set higher than when using the Keithley 236 (during the nickel measurement). This lead to a significant difference between the 'a' parameters of both measurements.

The problem has been worked around in Section 4. However, using the calibration parameters in the calculation means that we need to take a look at the errors of these parameters. The parameters were obtained using linear regression, this also yielded the following coefficients of determination for nickel and copper sulfate respectively:

- 0.9999985027
- 0.9998095329

Thus the error in the linear fit is relatively small.

Note that when using the box's battery as power supply for the potentiometer, it is still required to correct the reference if there is a large time delay between VSM calibration and measurement. This is due to the battery slowly depleting overtime, however if one records the current battery voltage for each measurement one can easily divide the reference signal by this voltage. Thus compensating for the battery drain and making the reference dimensionless. This has been done for all measurements after Section 4.

8.2 Magnetization at B is not the same as at -B?

The attentive reader might have noticed that in Figure 7 at saturation the signal for positive B is always below the average-line, while for negative B it is above. This appears to suggest that the saturation magnetization of the nickel sample is larger for negative magnetic field and smaller for positive magnetic field. This is of course impossible, something else must be going on!

A possible explanation for this aberration would be a constant negative DC offset in the VSM's signal. However the signal goes through a 4 Hz high pass so any DC offsets should have been filtered out.

Another potential explanation is that there is some small contribution to the overall magnetization by the sample holder or impurities left behind by previous samples in the holder (we know the holder's magnetization is non zero, Figure 8). However these components would have to have a magnetization that is somehow not the same for different directions of the magnetic field.

A satisfying explanation to this strange behavior has yet to be found. However by including both the contributions at negative and positive field in the average and standard deviation we include the difference between the two in the error.

Note that the same problem is also visible in the offset of the sample holder's linear fits as shown in Figures 11, 13 and 14.

8.3 Possibility for compensating for magnetization of empty sample holder

In determining the calibration constant (Section 3.3) we assumed that 0 sample magnetization corresponds to 0 signal. However if we look at Figure 8 we see that this is not entirely true, as the sample holder (and impurities left behind by previous samples) also have some small (diamagnetic) contributions to the overall magnetization.

A possibility to compensate for this exists in using 2 different samples (e.g. Nickel and Iron) with known magnetization for calibration and linear fitting those ($y = ax + b$ instead of $y = ax$). This removes the assumption that the calibration-line should go through the origin ($b=0$), and thus allows for some signal to exist at 0 field without it interfering with the measurement of some unknown magnetization later on. Note that the empty sample holder leads to a signal of the order of 0.01 (Figure 8) which is within the error (standard deviation: 0.002) of the copper sulfate measurement (Figure 10).

A better option is to do the exact same measurement without the sample, and thus in effect measuring the empty sample holder (Section 5) And then subtracting the linear fit of this background from all data points.

8.4 Different calibration parameters?

In Sections 3.3, 6 and 7 different calibration parameters were obtained. For Section 3.3 ($c=(29.34 \pm 0.06)$ emu) this is because the amplitude was different compared to the later measurements and because this calibration did not use a dimensionless reference (Section 8.1). The difference between Section 6 ($c=(3.6 \pm 0.2)$ emu/V) and Section 7 ($c=(7.8635 \pm 0.0004)$ emu/V) is explained by the fact that during the measurements in Section 7 the sample was not in between the coils. Instead it was in the local maxima of the lower coils (Figure 2). Because of this the VSM's sensitivity was halved, and the sample was not in the flat area (Figure 2). While this is not optimal, it is not a big problem for a sample with such a large response. The calibration parameter in Section 16 however is correct, for a sample in the center (flat area Figure 2). The reason the sample was not in the center is because when finding the center the local minimum was mistaken for the global maximum. To prevent this problem from occurring in the future, always check that the found maximum is wide enough to be the global maximum (flat area Figure 2). This can also be checked by measuring the contributions of individual pickup coils, if all of the signal is on the upper or lower pickup coils the sample is not in the global maximum but in a local minimum.

Acknowledgments

None of this would have been possible without the help of Prof. Dr. Uli Zeitler, who gave me the opportunity to work with the VSM at HFML. And was always there to answer my many questions, and to explain how all the things worked; the VSM, the lock-in amplifiers, the cryostat, the helium pump, and of course the bitter magnets. My sincerest thanks.

My thanks also to Hung van Luong, who taught me how to use the VSM control program and also showed my how all the devices (lock-ins, filters) should be connected to each other. And helped me whenever I had problems with the motor or the computer.

Furthermore, my thanks go out to Lijnis Nelemans, Michel Peters and Edwin van Leverink, who setup the VSM, helped me to create the potentiometer's box and provided me with technical advice and equipment.

To Anabel and Patrica from the University of Deusto (Bilbao, Spain) thanks for providing a very interesting sample, and explaining the physics behind the martensite/austenite phase transitions.

Also thanks to dr. Dmytro Kamenskyi and Bence Bernáth for providing yet another interesting sample.

I also would like to thank the rest of the amazing staff and students at HFML, who have been very kind and helpful in showing me around and helping me find all the things in the lab.

Thank you

References

- [1] A.A.L.N. Ammerlaan. *HFML-VSM pickupcoil profile plotter*. URL: https://github.com/AndrewAmmerlaan/HFML-VSM_CoilProfilePlotter.
- [2] *HFML magnet specifications*. URL: <https://www.ru.nl/hfml/facility/experimental/magnets/>.
- [3] O. Young. logbook.
- [4] E. Kampert. “Magnetic properties of organometallic compounds in high magnetic fields”. PhD thesis. Radboud University, 2012.
- [5] C. Kittel. *Introduction to Solid State Physics*. 8th ed. Wiley, Nov. 2004. Chap. 11,12.
- [6] H. Danan, A. Herr, and A. J. P. Meyer. “New Determinations of the Saturation Magnetization of Nickel and Iron”. In: *Journal of Applied Physics* 39.2 (1968), pp. 669–670.

A Using the VSM motor controller program

To start motor:

- **Warning:** If you disconnect the motor's powersupply, the motor will have to be reinitialized ("Init"). This means that the motor will have to be disconnected from the VSM, which usually means that both the potentiometer's calibration and the VSM's center will change. Hence a full recalibration is required.
- Press "Connect to VSM", usually the VSM resides on COMM 3, and the default settings are fine
- Press "Ok"
- If not already on, press "Motor on"
- If this is first time the motor is used after it has been plugged in: press "Init". The motor will move as far up as it can go, and use that as the zero position. For this to work, the motor has to be disconnected from the rest of the VSM, and the potentiometer must be moved all the way up.
- Set the desired frequency, displacement (2x amplitude), and begin position (the motor will vibrate between 'begin position' and 'begin position' + 'displacement').
- Click "Calculate freq code", this will convert the frequency and displacement into a single code that the motor can understand.
- Click "Send calc freq code", which will send the frequency code to the motor.
- Click "Send string", this sends the string that contains the 'begin position' parameter to the motor.
- Click "Start motor", to stop the motor click "Stop motor".

Starting a position loop:

- Complete the above, but do not yet start the motor.
- Set the desired step size, number of steps and step duration.
- Click "Start position loop"
- When the loop has been completed, the motor will continue to vibrate at the last position, to stop the motor click "Motor on" immediately followed by "Motor off"

Troubleshooting:

- Motor does not respond:
The motor stores commands in finite volatile memory, when it is full the motor cannot receive any further commands from the controller program. To clear the memory, press the buttons "Flush input queue", "Flush output queue", and "Reset macro".
- Motor does not start:
If the motor does not start after it has been disconnected from the power, press "Init" to reinitialize the motor. Because the motor uses volatile memory, it will forget everything once the power has been disconnected.
- Motor still does not start:
Try to start the motor without anything attached to it. If it works now, it is because there was too much friction. Try adjusting the potentiometer, or turn the connector piece a bit.
- The motor stops halfway a position loop:
Beyond this point the motor encounters too much friction to continue, sometimes the friction can be reduced by turning the connector piece a bit for optimal alignment.

B VSM measurement step-by-step

Initial setup

- Put cryostat in magnet, and put VSM inside cryostat.
- Adjust VSM height (Figure 20) such that the pickup coils are in the center of the external magnet (Measure the distance from top of cryostat to the center of the magnet, and use schematics in appendix C).
- Connect lock-ins/amplifiers etc. as shown schematically on page 29.
- Connect cryostat to the lakeshore 350 and to the helium pump. Connect the VSM's thermometer to the lakeshore as well.
- Set the calibration curves the lakeshore should use for the thermometers (VSM:x07377, cryostat2:46682).
- Vacuum pump the cryostat's vacuum chamber.
- Setup measurement program to record signal, AC-reference, DC-reference, temperature and magnetic field
- Move potentiometer all the way up.
- Turn the motor on, and initialize (Appendix A), if not already initialized.
- Turn the motor off.

Putting a sample in the VSM

- Put calibration sample in sample holder, and screw it onto the sample stick (Figure 21b).
- Screw the sample stick onto the connector piece (Figure 21a), and put the stick in the VSM.
- Connect the motor to the connector piece.
- Adjust the connector piece such that the motor can move freely (Try screwing the connector piece tighter/looser), when done correctly the motor will fall down when pushed up and released.
- Move potentiometer such that the motor can make use of the full range of the connector piece.
- Turn motor on
- Find the smallest and largest possible motor position, do this by choosing some position and visually checking the connector piece.
- Calibrate the potentiometer, by setting the motor to a couple of different begin positions and writing down the corresponding DC component of the reference, and making a linear fit.

Cooling sample

- Fill cryostat with liquid nitrogen followed by liquid helium, depending on desired temperature.
- If required set desired temperature in the lakeshore and enabled the heater.
- Once desired temperature has been reached turn on the motor and the bitter magnet.

Doing a measurement

- Set the motor to vibrate at some position, and set the bitter magnet to some field where there is a clear signal, adjust signal/reference amplification if required. Note that for calibration samples that already have a magnetization the bitter magnet can stay off for the time being.
- Use the lock-in's "autophase" function
- Do a position loop from the smallest to the largest position. To save time it might be a good idea to first do a rough position loop with large steps, and finding where the center is approximately. Followed by a second more detailed position loop, with more steps, using an educated guess as begin position. Use coilprofileplotter.py to help find the center, detailed instructions in the readme file [1].
- Double check that the found center is in fact correct, by checking that both the upper and lower coils give equal contributions to the signal. If the found center is incorrect, the lower or upper coils do not give any signal, shorten/lengthen the sample stick as required.
- Set the motor's begin position and displacement such that the sample will vibrate exactly in between the pickup coils.
- Measure as a function of the magnetic field.

Replacing sample

- Turn off the motor, and disconnect it from the connector piece.
- Create a over-pressure in the cryostat, unscrew the connector piece and remove the sample stick, then put the connector piece back on the VSM.
- Replace sample in sample holder.
- Unscrew the connector piece and reattach the sample stick, screw the connector piece back on the VSM and reconnect the motor.
- Wait for sample to reach desired temperature.
- Re-calibrate the potentiometer, and do a new position loop.

Calibrating VSM

- Steps "Putting a sample in the VSM" and "Cooling sample" for calibration sample.
- Steps "Doing a measurement".
- For better calibration: Steps "Replacing Sample" with second calibration sample, or measure the empty sample holder.
- For better calibration: Steps "Doing a measurement".
- Identify the saturation point(s) and find the relative absolute signal(s) at saturation.
- Use the known magnetization of the calibration sample(s) to obtain a calibration ' $c*x$ ' or ' $c*x+b$ '.

Measuring sample with unknown magnetization

- Steps "Replacing sample" for target sample.
- Steps "Doing a measurement"
- Identify saturation point and find the relative absolute signal at saturation, make sure to correct the reference first using the ratio of the battery voltages (if changed).
- Use calibration to find magnetization and magnetization per gram.

C Schematics and Pictures

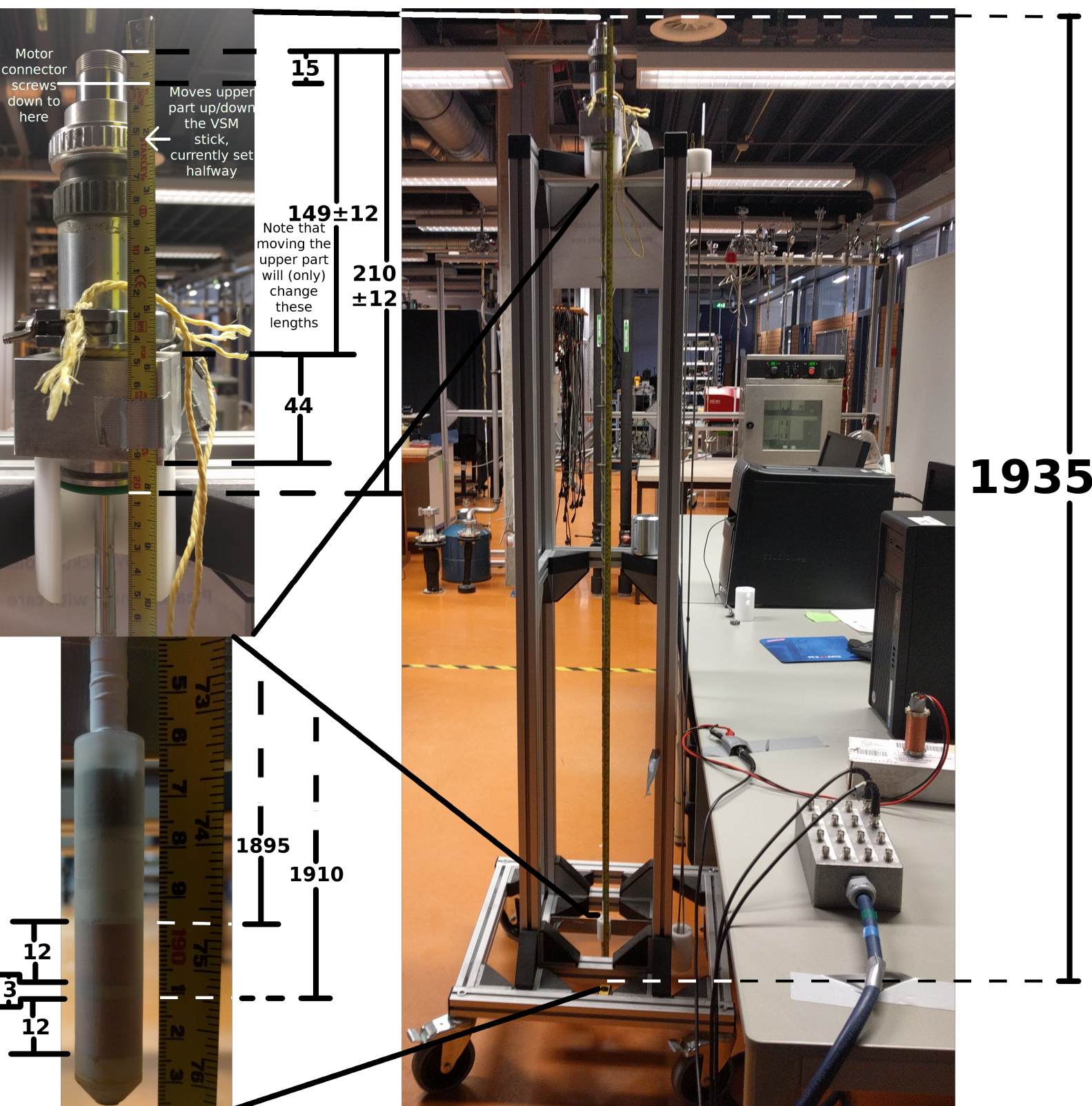


Figure 20: At room temperature, lengths (mm) will depend on temperature.

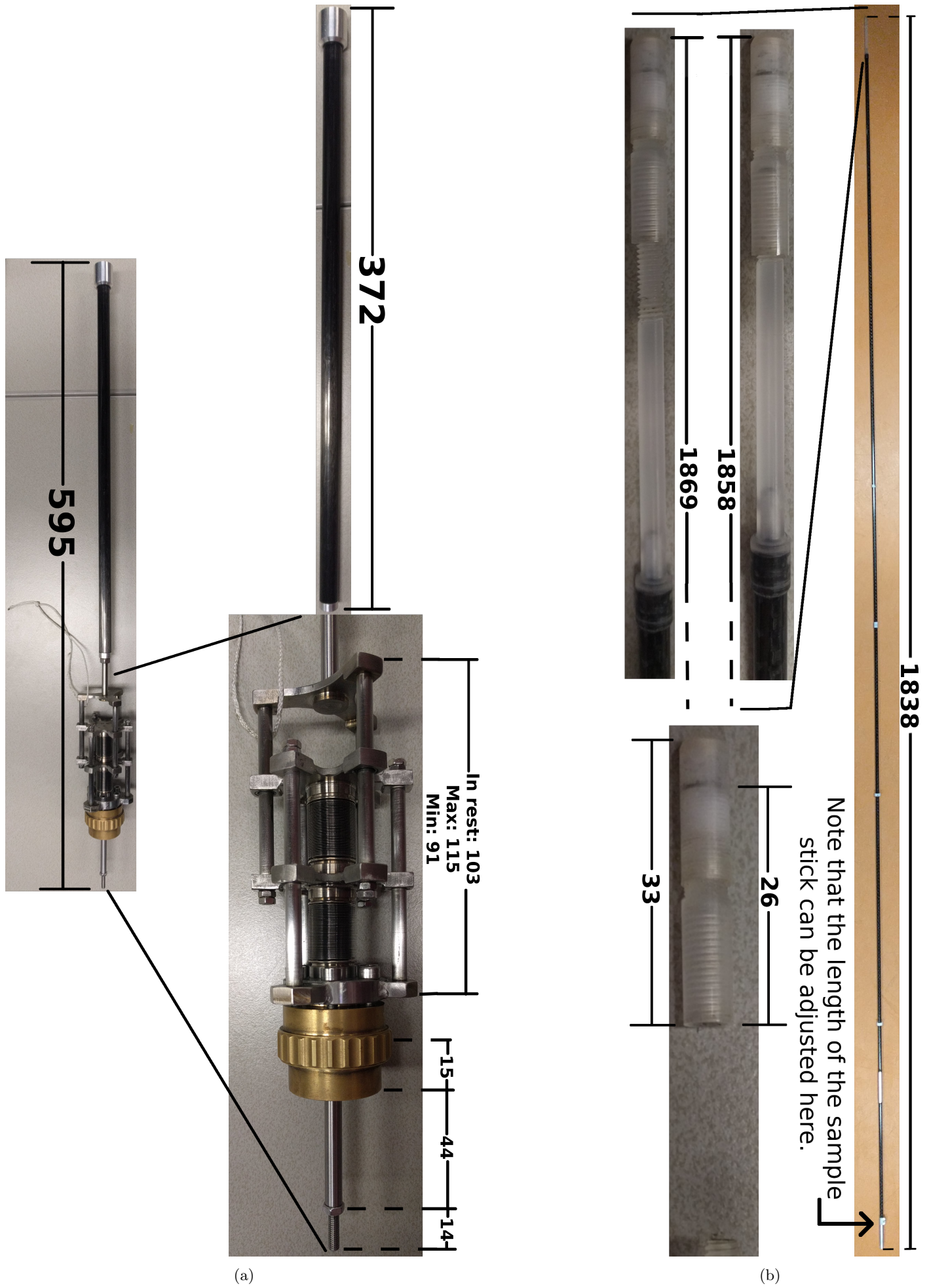


Figure 21

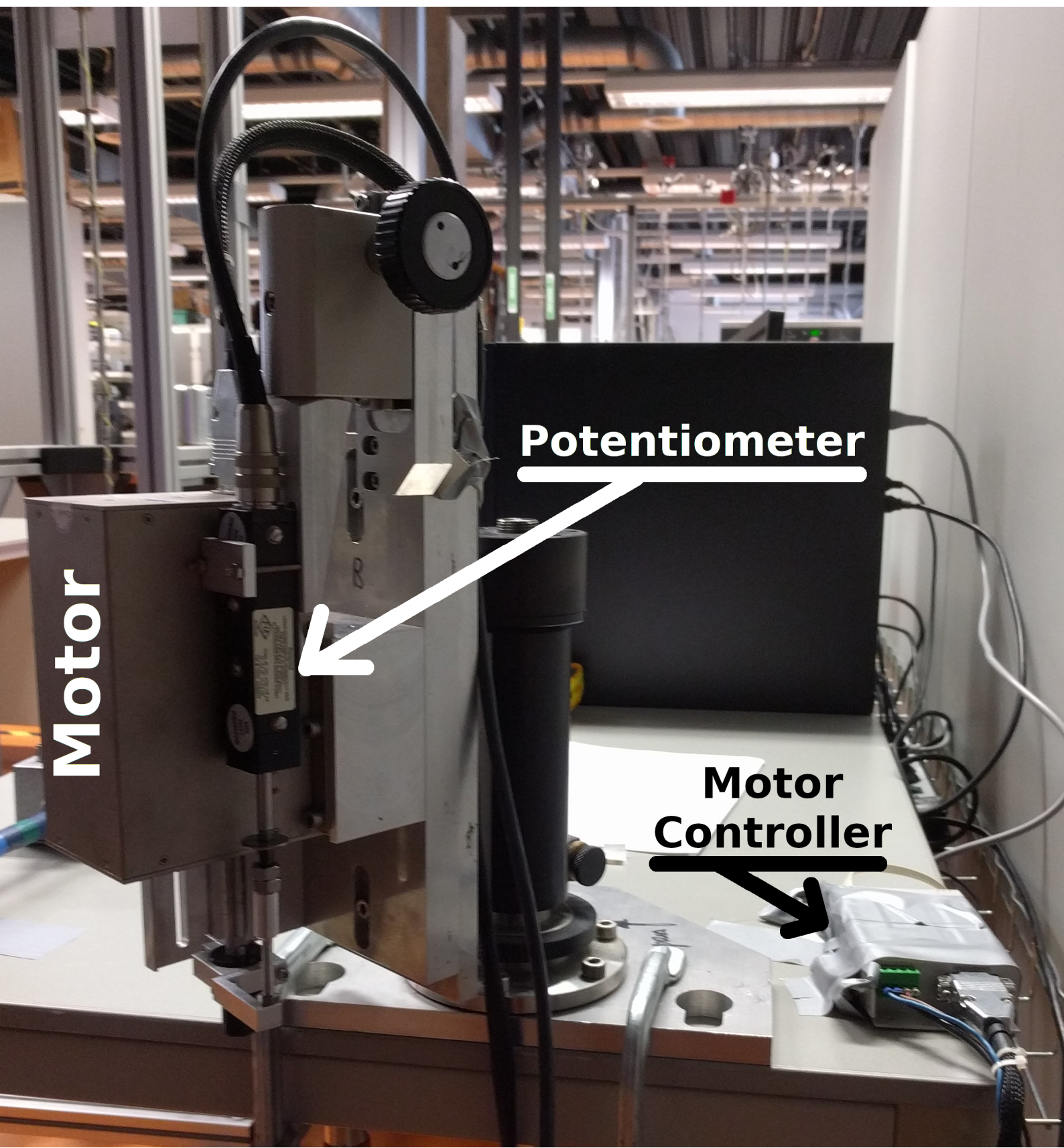


Figure 22

